Chapter 3

Directional cues affect the collective behaviour of Self propelled particles in one dimension

3.1 Introduction

In chapter 2, we discussed the phase transition in collective behaviour of polar flocks with birth and death. In this chapter we discuss ordering in the polar flocks in one dimensional system with inhomogeneity. Most of the previous studies on the dynamic and steady-state properties of active matter systems focus on systems in clean or homogeneous media [Pattanayak & Mishra (2018a); Toner & Tu (1995, 1998b); Toner et al. (2005b)]. However, disorder or inhomogeneity is inevitable in nature [Chepizhko et al. (2013); Mishra & Mishra (2023); Morin et al. (2017b); Reichhardt & Reichhardt (2017); Yllanes et al. (2017)]. Some recent studies have shown the effect of disorder on the ordered state of polar self-propelled particles in two and three dimensions [Chepizhko et al. (2013); Das et al. (2018b, 2020); Kumar & Mishra (2020b, 2022); Kumar et al. (2021b); Morin et al. (2017b); Pattanayak et al. (2020); Quint & Gopinathan (2015); Sándor et al. (2017a); Singh et al. (2021a,b); Yllanes et al. (2017)]. It is observed that disorder can break the robust long-range ordered state in two dimensions and change it to quasi-long-range order [Das et al. (2018a)], whereas in three dimensions, the ordering remains unaffected by the presence of disorder [Toner et al. (2018a)].

The presence of long-range ordered states in clean systems i.e. active systems without heterogeneity or disorder sources is also observed not only in two and higher dimensions but in one dimension as well. A natural way of observing such long-range ordering in one dimension can be seen in moving ant trails [Attygalle & Morgan (1985); Goss et al. (1990)], or traffic flow in a single lane [Herman & Potts (1959); Wang et al. (2007)]. The long-range ordering of one-dimensional wires is observed in quasi-1D systems [Mamiyev et al. (2021)]. This motivated us to investigate the role of disorder in the collection of active agents in one dimension.

Understanding the behavior of active systems in 1D channels under the influence of disorder or directional cues is not only theoretically interesting but also practically significant. Systems such as bacterial motion in microfluidic channels [Männik et al. (2009); Vizsnyiczai et al. (2020)], motor proteins moving along filaments, and vehicular traffic on single-lane roads all exemplify 1D active matter in the presence of disorder. For example, bacteria in microfluidic channels often encounter irregularities and varying chemical gradients that act as directional cues, affecting their movement and collective behavior. Similarly, motor proteins experience fluctuations in the filament structure and binding sites, leading to variations in their transport efficiency. In vehicular traffic, obstacles, and irregularities on the road or varying traffic signals serve as directional cues, impacting the flow and causing clustering or jams. These systems are important for various applications, including the design of efficient microfluidic devices that can control bacterial movement despite channel imperfections, optimizing traffic flow in the presence of road irregularities, and understanding intracellular transport mechanisms under fluctuating conditions.

In our study, We strictly maintain that the nature of the disorder only influences the direction of incoming particles. This type of disorder acts as a field that is not physically present and does not obstruct the path of the incoming particles, thus serving as *directional cues*. Any other type of physical disorder would block the path of particles and immediately break the clustering and ordering among the particles. Our findings contribute to answering how directional cues in a disordered environment affect the collective behavior of self-propelled particles in one dimension. This is relevant for understanding natural phenomena like ant trail formation and traffic flow and has potential applications in designing synthetic systems with desired collective behaviors.

We model our system as a collection of active agents moving on a one-dimensional ring (due to periodic boundary condition) with short ranged alignment interaction with the neighbouring particles as well as with the disorders placed random in space with ± 1 orientation and quenched in time. For zero disorder we find the macroscopic clustering and the presence of disorders splits the macroscopic clusters and lead the local trapping of a moving particles. For all disorder densities the two-point orientation correlation function shows a mixture of algebraic and exponential decay. The cluster size algebraically decreases with the density of disorder. System shows good dynamical scaling for all disorder densities. Results obtained from microscopic simulation and coarse-grained model are in good match with each other.

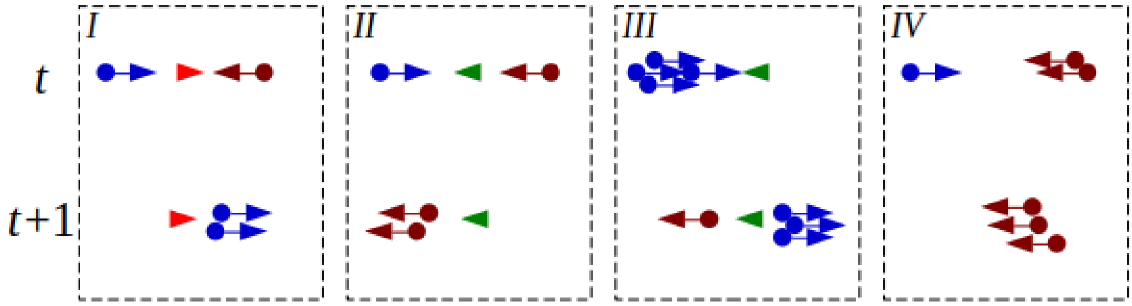

Fig. 3.1 In this illustrative diagram, all the possible scenarios of the flipping of SPPs are showcased in different panels. (I-III) represent when there is a disorder in the path of SPPs, (IV) when there is no disorder is present. SPPs and loactions of disorders are depicted as a circular entity connected with an arrow, right-moving SPPs are marked in blue, while left-moving ones are portrayed in brown. Similarly, quenched disorders within the system are illustrated with an arrowhead; left and right-oriented disorders are marked in green and red, respectively. The SPPs and disorders in the top row are shown at a particular time t before the interaction with SPPs/disorders and in the bottom row at time $t+1$ after the interaction with SPPs/disorders.

3.2 Model and Numerical Methodology

Microscopic Model:- We study a collection of self-propelled particles with discrete symmetry in one-dimension in the presence of disorder. Disorders, which are placed random in space and quenched in time act like *directional cues*. We have considered N (N_d) particles (disorders) placed randomly along a line of length L. Hence the number density of particles(disorders) $\rho(\rho_d) = \frac{N(N_d)}{L}$, where $N_d << N$. The position and orientation of i^{th} particle at time t are given by $x_i(t)$ and velocity $u_i(t)$. The configuration of directional cues is quenched and they are randomly placed in space with random orientation ± 1. The position and velocity of the particle is updated by

$$x_i(t+1) = x_i(t) + v_0 u_i(t) \tag{3.1}$$

$$u_i(t+1) = G(\langle u(t) \rangle_i) + \xi_i \tag{3.2}$$

$\langle u(t) \rangle_i$ is the local average velocity of particles and disorders around the i^{th} particle [Czirók et al. (1999)]. It is calculated by averaging over the particles and disorder in the interval $[x_i - \Delta, x_i + \Delta]$ with $\Delta = 1$, $\xi_i \in [-\frac{\eta}{2}, \frac{\eta}{2}]$ is the random white-noise uniformly distributed between $-\eta/2$ to $+\eta/2$. This is due to any kind of randomness present in the system. The strength of noise η is set such that the system without directional cues or the clean system is in the ordered state [Czirók et al. (1999)]. We fixed the $\eta = 1.0$. The parameter v_0 controls the self-propelled nature of the particles. We fix the magnitude of v_0 to 1.

$$G(u) = \frac{u+1}{2} \quad \text{for} \quad u \geq 0; \quad \frac{u-1}{2} \quad \text{for} \quad u < 0 \tag{3.3}$$

In the presence of disorder, the

$$\langle u \rangle_i = \sum ((u_j + \beta u_j{}')/n_r) \tag{3.4}$$

u_j and $u_j{}'$ are the velocity of particles and orientation of directional cues respectively in the interaction radius of i^{th} particle. β controls the strength of interaction with directional cues. We fixed the $\beta = 10$, such that disorder interacts strongly with particles and interesting results can be obtained for the finite range of disorder and particle densities. n_r is the number of particles and disorders in the interval $[x_i - \Delta, x_i + \Delta]$. The disorders which have either left or right orientation, try to reorient the particles in their direction. The cartoon of the effect of orientation interaction; the first term on the right hand side of Eq.(5.2) for four different scenarios is shown in Fig.[3.1]. Fig.[3.1](I)-(II) shows the disorder acting like transmitter/reflector when the direction of incoming particle is same/opposite to the direction of disorder. Fig.[3.1](III) shows a big cluster of particles interacting with disorder with the direction of disorder opposite to the direction of incoming cluster,causing the big cluster to split and a fraction of particles from the cluster getting reflected and another part getting transmitted. Fig.[3.1](IV)shows the scenario when a cluster of particles interact with another particle and no disorder is present at that location, then the majority wins and a bigger cluster is formed. For clean system or for zero disorder $\rho_d = 0$, model reduces to the model introduced by Czirók et al. (1999). We name this case as *pure system*. The other parameters in the system, particle density $\rho = 1$, system $L = 2000$

Coarse Grained Model:- We further introduce the coarse-grained model for the collection of self propelled particles with quenched disorders in one dimension. We define the coarse-grained fields by dividing the whole system in units of size 2Δ. The local coarse-grained density and magnetisation is defined as $\rho(x,t) = \frac{N_x(t)}{2\Delta}$, where $N_x(t)$ is the number of particles at the lattice point x in the interval $[x - \Delta, x + \Delta]$ and $m(x,t)$ is obtained by taking average orientation of all the particles in the same interval at time t. The effect of disorder is added as an additional noise which is random in space and quench in time. The equations of motion for the coarse-grained density $\rho(x,t)$ and magnetisation $m(x,t)$ are given by

$$\partial_t \rho = D\partial_x^2 \rho - v_0 \partial_x (m\rho) \tag{3.5}$$

$$\partial_t m = D\partial_x^2 m - v_0 \partial_x (\rho) + (\alpha(\rho) - \alpha_2 m^2)m + f_m + \xi \tag{3.6}$$

The first terms on the right hand side of Eq.(3.5) is the diffusion in density, the second term is the term due to self-propelled nature of particle, where the active current is proportional to the local magnetisation m. The first term on the right hand side of Eq.(3.6) is again the diffusion in magnetisation, the second term is the coupling due to density inhomogeneity and present due to self-propelled nature of particles. The third term is usual order-disorder term, where region with high density promotes ordering and regions with low density favours random orientation. Such density dependent order-disorder coupling is introduced by taking $\alpha(\rho) = (\frac{\rho}{\rho_c} - 1)$. Hence it changes sign at $\rho = \rho_c$. α_2 is a positive constant. The second last term f_m is the random annealed Gaussian white-noise with mean zero and strength Δ_m, such that $\langle f_m(x,t) f_m(x',t') \rangle = 2\Delta_m \delta(t-t')\delta(x-x')$. This term is present due to randomness in the system, which acts like thermal noise in the coarse-grained model. The last term is the effect of disorder and it is introduced as an additional Gaussian white-noise; quenched in time and random in space with mean zero and strength $\Delta_d = \frac{\rho_d}{\rho_0}$, where ρ_d is analogous to disorder density in the microscopic model and ρ_0 is the mean density of particles in the system. The noise-noise correlation is $< \xi(x)\xi(x') >= 2\Delta_d \delta(x-x')$. Hence the strength of noise Δ_d controls the density of disorder in the system. To control the effect of disorder the Δ_d is varied from $(0, 0.001 - 0.007)$. For $\Delta_d = 0$, the model reduces to the clean system and it is analogous to the one-dimensional limit of the *Toner-Tu* equation for polar flock [Toner & Tu (1995, 1998b)]. We numerically integrate the two equations Eq.(3.5) and Eq.(3.6) using Euler's scheme in one-dimension of system size L with periodic boundary condition. The intrinsic length scale and time scale of the system is chosen to be $l_0 = 1$ and $\tau = 1$. Here we employ the euler discretization scheme with mesh sizes $\Delta x = 0.5l0 = 0.5$ and $\Delta t = 0.01\tau = 0.01$ where the spatial interface is taken such that the coarsening interfaces can be smoothly treated and the temporal discretization is chosen so as to maintain the stability of the numerical scheme. We start from a randomized and homogenous state with initial number density $\rho =< \rho > 0.05$, wherein $\rho_0 = 0.6$ and $\rho_c = 0.1$. We have studied these conditions on a system size $L = 1024$. Before the start of the simulation we checked that the given Euler discretization scheme with chosen parameters is stable for a system with disorder.

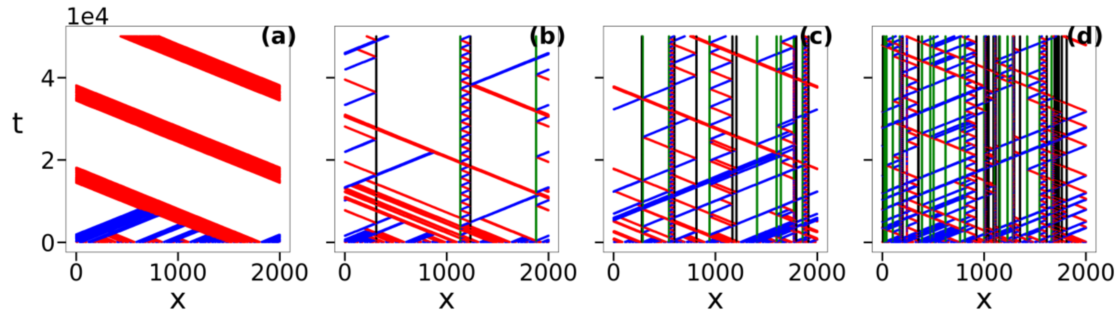

Fig. 3.2 In this series of spatio temporal snapshots (a)-(d) for $\rho_d = 0, 0.002, 0.008$ and 0.02 respectively, the one-dimensional system unfolds over time, where the x-axis represents the spatial coordinates of SPPs and disorders. The y-axis signifies the progression of time. SPPs with leftward orientation are depicted in red, while those with rightward orientation are shown in blue. Left-oriented obstacles are represented in green, and right-oriented obstacles in brown.

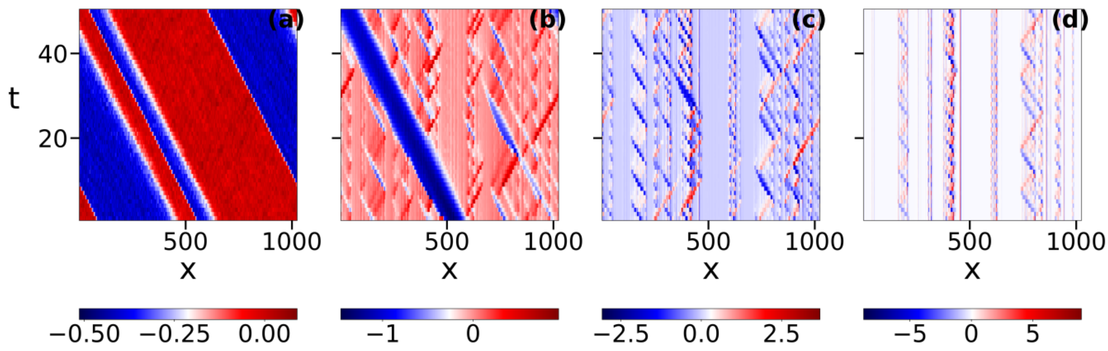

Fig. 3.3 The spatio-temporal snapshots (a-d) illustrates the effect of increasing the disorder strength $\Delta_d = (0, 0.001, 0.01, 0.04)$ respectively in the coarse-grained model. The $x-$axis denotes the product of local magnetization and density $g(x,t)$ and the $y-$axis represents the increasing time direction. The color bar represents the value of $g(x,t)$

3.3 Results

To understand the effect of disorder in the system we first plot the spatio-temporal plot of local density and magnetisation for different densities ρ_d and strengths Δ_d of disorder in microscopic and coarse-grained models respectively. Fig.[3.2](a-d) shows the spatio-temporal plot of particle's position in the microscopic model. The two colors show the two types of orientation of particles; red color represents the left orientation and blue color shows the right orientation. The first plot in Fig.[3.2](a) is for the zero disorder or clean system and shows the macroscopic ordering in the system. The vertical direction shows the flow in time and horizontal axis is the system dimension. It is very clear that for the clean system initially there are clusters of different orientations and with time the clusters merge and a big macroscopic cluster is formed and moves coherently in the direction of its orientation. The direction of motion of the cluster is spontaneously chosen in the system. The Fig.[3.2](b-d) shows the same plot in the presence of disorder and for different disorder densities. Fig.[3.2](b) is for small density of disorder $\rho_d = 0.001$. It is clear that the disorder affects both the ordering and clustering in the system. When an incoming trail of particles encounter a disorder, it tries to get reoriented (due to alignment interaction with disorder Eq.(3.4)) in the direction of disorder. If the size of the trail is large, and the direction of disorder is opposite to its incoming direction, then a part of it can get reflected and some part can be transmitted. This is scenario when disorder density is small. As we increase disorder density, then a moving particle cluster encounter with disorder more frequently and it leads to the breaking of a big cluster into many small clusters. Many times these small clusters are simply stuck between two oppositely oriented disorder. Hence the macroscopic clustering in the system is broken and big cluster splits in clusters of different orientation and high density (narrow bands). On increasing disorder as shown in Fig.[3.2](c-d), the cluster of particles splits in many small clusters and many times these clusters perform the back and forth motion between two oppositely oriented disorder and essentially lead to the local trapping of particles between two oppositely oriented disorders. Hence a small cluster of particles are trapped. Which can be very clearly seen in zig-zag motion of particles between disorders of opposite orientation as can be seen by two vertical lines of different colors.

Similarly we make the spatio-temporal plot of the local magnetisation density $g(x,t) = \rho(x,t)m(x,t)$ for the coarse-grained model for different strengths of disorder Δ_d. The corresponding snapshots are shown in Fig.[3.3](a-d) for four different disorder strengths including clean system $\Delta_d = 0$. Clearly for the clean system as shown in Fig.[3.3](a), macroscopic clustering is observed with one big cluster moving in the direction of local magnetisation. Color bars in Fig.[3.3] show the value of $g(x,t)$ which denotes the variation of the local magnetisation density. If $g(x) > 0$, majority particles are moving in right direction while for $g(x) < 0$, they are moving towards left. As we increase the strength of disorder macroscopic clustering breaks and small denser clusters are formed, as can be seen by the range of the color bar for different strengths. Since the local magnetisation $m(x,t)$

can only vary between ± 1, hence increasing color bar mean local density has increased. Further larger magnitude of $g(x,t)$ is found in small narrow regions, that can be due to the locally high disorder strength in that region. Hence increasing disorder leads to increase in particle density in the clusters rendering them immobile. From the Fig.[3.3](b-d) and [3.2](b-d) we can say that the disorder not only splits the clustering and breaks the ordering but also creates the localisation of particles.

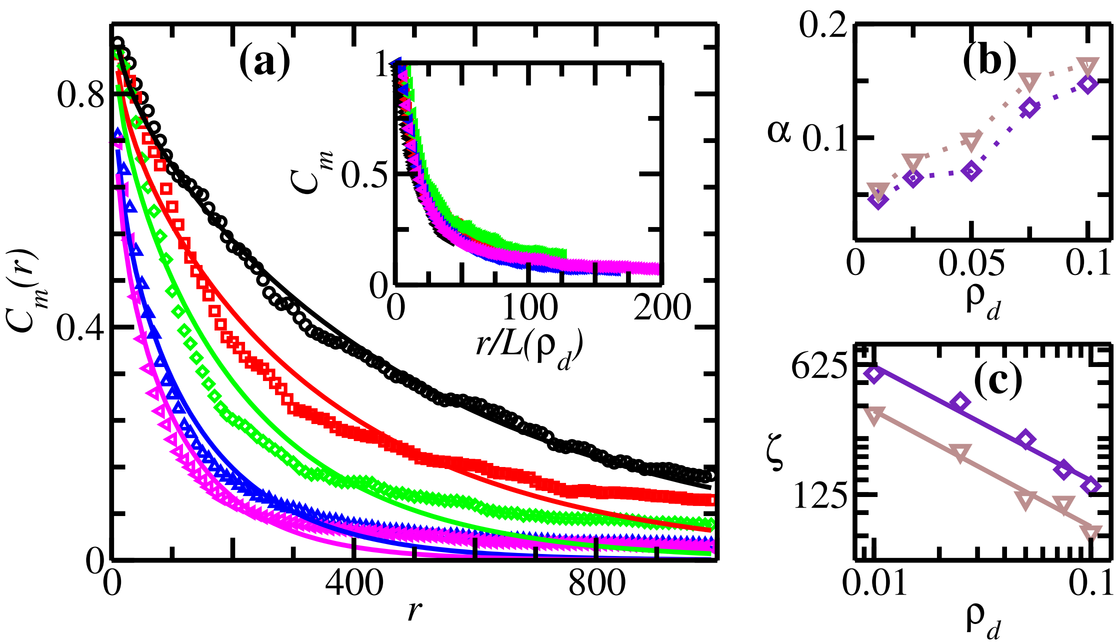

Fig. 3.4 (a) Two-point Spatial correlation function $C_m(r)$ *vs.* r for different disorder densities (ρ_d = 0.010, 0.025, 0.050, 0.075 and 0.100) for microscopic model in the steady state at time $t = 12000$. The symbols are data from numerical simulation and lines are fit to the proposed form of the $C_m(r)$ as given in Eq.(5.1). *Inset*: The plot of scaled $C_m(r$ *vs.* scaled distance $r/L(\rho_d)$ for different disorder densities. Plot (b) shows the power exponent $\alpha(\rho_d)$ *vs.* ρ_d on linear scale. The two symbols show the power exponent for different packing fraction of the SPPs/disorders along the fixed length, violet square is for density 1.0 while brown triangle for particle density 2.0. (c) Demonstrates the cluster size $\zeta(\rho_d)$ *vs.* ρ_d on log − log scale. Symbols have usual meaning as in (b).

Till now, we have discussed the impact of disorder through spatio-temporal snapshots of the system, which suggest that disorder splits a large macroscopic cluster into a greater number of smaller clusters with relatively high density due to the local trapping of particles. This observation holds true for the density field of particles. However, disorder also affects the orientational ordering within the system, as shown in Fig.[3.4]. The effects on local density and orientation are coupled, as described in the coupled coarse-grained

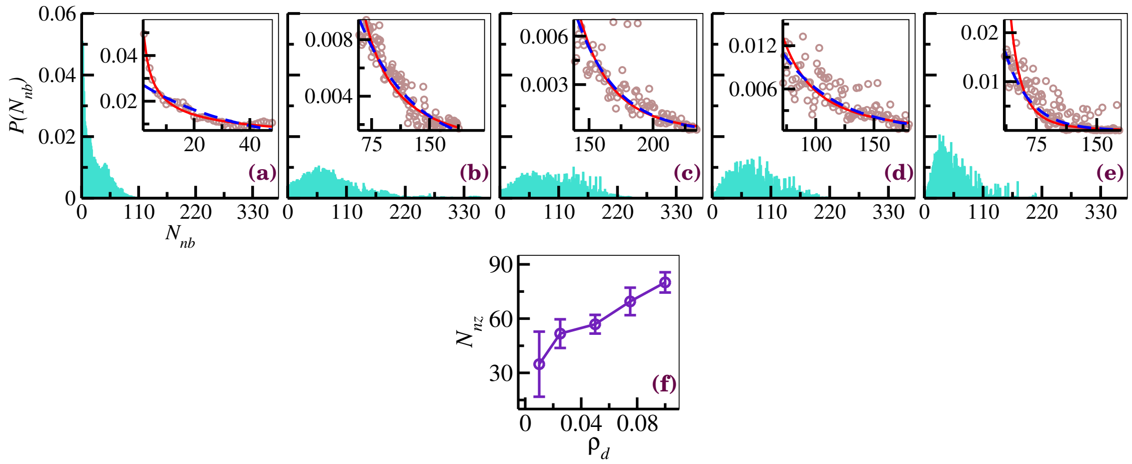

Fig. 3.5 (a)-(e) show the distribution neighbours for ρ_d = 0.010, 0.025, 0.050 and 0.100 respectively. (a)-(e) insets show the fitting of corresponding distribution of neighbours by power law (red) and exponential (blue). (f) Plot of number of cells with non-zero densities N_{nz} with respect to disorder density ρ_d.

hydrodynamic equations of motion for the two fields. We further characterize the system by calculating the two-point magnetization correlation function. First, we focus on the results for the two-point correlation function obtained from the microscopic model. The two-point magnetization correlation function is defined as

$$C_m(r) = \langle \vec{u}_i \cdot \vec{u}_j \rangle_r, \tag{3.7}$$

where i and j are indices for pairs of particles, and $\langle \cdot \rangle_r$ indicates an average over all (i, j) pairs separated by distance $r \pm \Delta r$. Furthermore, the correlation is averaged over 40 independent realizations.

In Fig.[3.4](a), we show the variation of $C_m(r)$ as a function of distance r for different disorder densities $\rho_d = 0.010, 0.025, 0.050, 0.075$, and 0.100, with particle density $\rho = 1.0$ in the steady state. As shown in the snapshots in Fig.[3.2](a) and (b), disorder breaks a large macroscopic cluster into smaller clusters, thereby destroying long-range ordering. Fig.[3.4](a) illustrates that $C_m(r)$ decays with distance r for different levels of disorder, with increased disorder leading to a sharper decay of $C_m(r)$ as a function of distance.

Upon analyzing the form of the two-point correlation function, we find that it is neither purely exponential nor purely power-law. Instead, it appears to be a combination of algebraic and exponential decay. The form of two-point correlation function is simply motivated by the quasi-long-range ordering disordered system in two-dimensions at small and moderate disorders and short ranged ordering at large disorders as can be found in [Das et al. (2018a)]. Hence we used the combination of two types of correlation function, assuming one-dimensional system with random force field disorder is in-between these two. Thus, we propose a form for the two-point correlation function

$$C_m(r) = \frac{1}{r^{\alpha(\rho_d)}} \exp(-r/\zeta(\rho_d)) \tag{3.8}$$

where the exponent $\alpha(\rho_d)$ for the power-law and the cluster size $\zeta(\rho_d)$ are functions of disorder density ρ_d. We obtained the $\alpha(\rho_d)$ and $\zeta(\rho_d)$ by fitting the $C_m(r)$ with the proposed form. In Fig.[3.4], lines are fitting functions and data points are obtained from numerical simulation. For all the cases we find the good fit of the $C_m(r)$ with respect to the proposed form of the correlation. In the Fig.[3.4](b-c) we show the variation of $\alpha(\rho_d)$ and $\zeta(\rho_d)$ *vs.* ρ_d on linear and $\log-\log$ scale for two densities $\rho = 0.5$ and 2.0. It is very clear that the $\alpha(\rho_d)$ increases linearly with disorder density and $\zeta(\rho_d)$ decays algebraically with ρ_d with $\zeta(\rho_d) \simeq \frac{1}{\rho_d{}^{\beta}}$. From the fit we found $\beta \simeq 0.61$. We further check the results for other particle densities. For all the densities we find the good fit of the $C_m(r)$ with respect to the proposed form for the correlation (data not shown). Comparing the orientation correlation with the density distribution in the system we can say that disorder splits a macroscopic globally ordered cluster (large $\zeta(\rho_d)$) and small N_{nz} to many localised dense clusters with different orientations (small $\zeta(\rho_d)$) and large N_{nz} and multiple peaks in number distributions $P(n)$ as shown in Fig.[3.4](a-e).

Further we also check the static scaling of the two-point correlation function by showing the scaled plot of $C_m(r)$ vs. scaled distance $r/L(\rho_d)$ in Fig.[3.4](a)(*inset*), where $L(\rho_d)$ is obtained by 0.1 crossing of $C_m(r)$. Very clearly good static scaling is observed for all disorder densities. Such scaling of data suggest the scale invariance of two-point correlation function for all disorder densities.

We now turn our attention to the effect of disorder on local density, and also show the distribution of the number of interacting neighbors n around a given particle for different densities of disorder ρ_d in the microscopic model. It is evident that for the clean system, the distribution shown in Fig.[3.5](a), the peaks at small densities, reflecting the presence of empty regions in the snapshots in Fig.[3.3](a). Additionally, the distribution shows a power-law tail (inset), representing the connected number of neighbors for each particle. Since the neighbors are connected, the system exhibits microscopic or long-range ordering. Upon introducing disorder, as seen in Fig.[3.5](b), the distribution broadens, indicating the breakup of a macroscopic cluster into multiple smaller clusters. The tail of the distribution also starts to deviate from a power-law (inset), indicating that different clusters are no longer connected, reducing orientational ordering as the correlation length decreases in Fig.[3.4](c). As the density of disorder increases (Fig.[3.5](c-e)), the distribution begins to shrink but maintains a finite value at moderate densities, with the height of the distribution increasing at these densities. This behavior suggests the presence of multiple small clusters with finite density, and the tail of the distribution becomes more exponential (insets of Fig.[3.5](c-e)). Consequently, ordering further decreases, and the correlation length monotonically decreases with ρ_d.

The presence of multiple clusters can be confirmed by counting the regions where a non-zero number of particles is found. Fig.[3.5](f) shows the plot of the number of bins N_{nz} with non-zero particles as a function of ρ_d. For this plot, the entire system is divided into bins of unit size, and the number of particles in each bin is calculated. Finally, N_{nz} is obtained by averaging the number over 10 different ensembles and over time in the steady state. (Note: Add error bars to this plot.) The value of N_{nz} shows a monotonic increase with disorder density ρ_d. Now we check the ordering kinetics and dynamic scaling of the

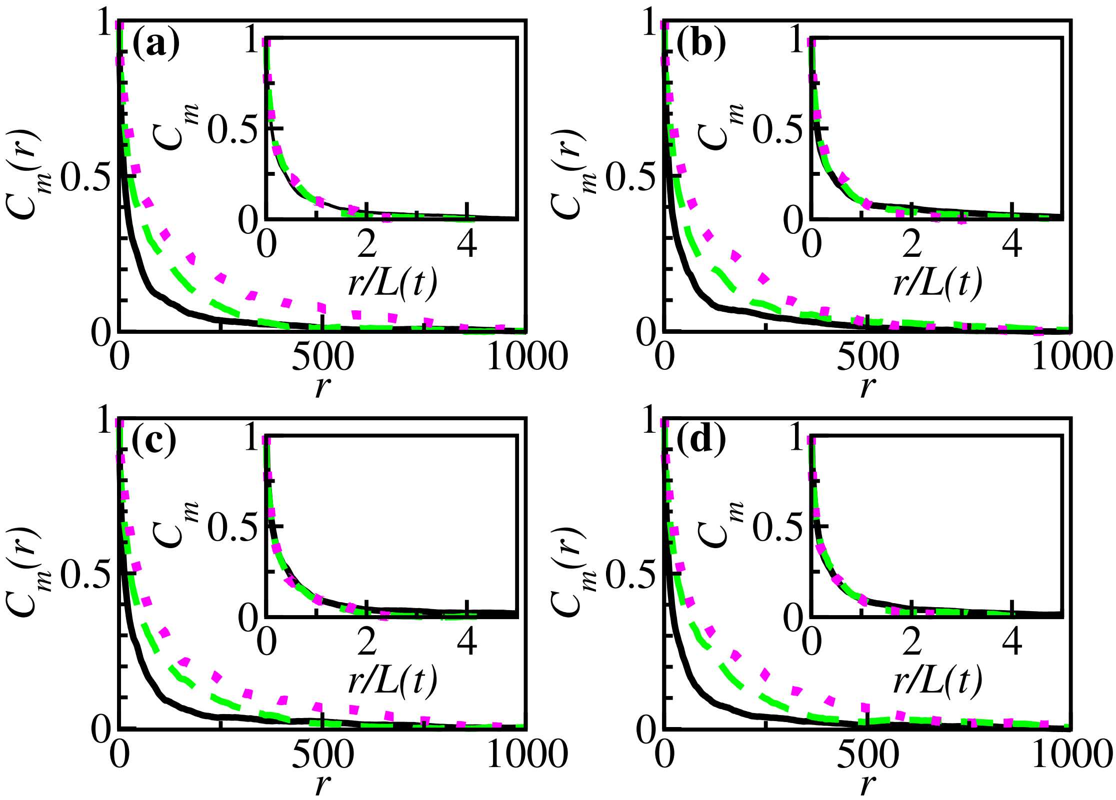

Fig. 3.6 Two point correlation function $C_m(r)$ *vs.* r at different times $t = 500, 1000, 1500$ shown by black (solid line) green (dashed line) and mazenta (dotted line) respectively and disorder densities $\rho_d = 0.010, 0.025, 0.050$ shown in different panels from $a-d$ respectively. *Insets*: The scaled $C_m(r)$ *vs.* scaled distance $r/L(\rho_d)$ for all the four cases.

two-point correlation function using microscopic simulation. In Fig.[3.6](a-d),we show the plot of $C_m(r)$ *vs.* r for four different disorder densities $\rho_d = 0.010, 0.025, 0.050, 0.100$ respectively and three different times $t = 500, 1000, 1500$. For all disorder densities, the correlation increases with time, which suggest the growth of clusters. Further the insets of Fig.[3.6](a-d) shows the scaling collapse of the same data as shown in the main panel. The correlation length is obtained by 0.1 crossing of the $C_m(r)$. For all disorder densities we find good dynamic scaling.

Further we also compared the two-point correlation function calculated in the coarse-grained simulation $\mathscr{C}_{cg}(r) = \langle \delta m(r_0,t)\delta m(r+r_0,t)\rangle_{r_0}$, where $\langle .. \rangle$ means average over many reference points and over 100 independent realisations. $\delta m(r,t)$ is the fluctuations in $m(r,t)$ from the mean value. Where mean is calculated by averaging over all points. In Fig.[3.7](a-b) we show the plot of $\mathscr{C}_{cg}(r)$ vs. distance r for different strengths of disorders $\Delta_d = 0.001, 0.002, 0.004$ and 0.007 in the steady state and for disorder strength 0.001 at different times respectively. In Fig.[3.7](a), the lines are the fit of the correlation function with the combination of power-law and exponential as proposed in Eq.(5.1) and symbols are from the coarse-grained numerical simulations. For a fixed time and increasing disorder the correlation steepens Fig.[3.7](a) and for fixed disorder and increasing time correlation increases with time Fig.[3.7](b). Hence the size of the ordered region increases with time. We calculated the correlation length $L(t)$ by the first 0.1 crossing of $\mathscr{C}_{cg}(r)$ and in the insets of Fig.[3.7](a-b) we show the scaled correlation function $\mathscr{C}_{cg}(r)$ *vs.* scaled distance $r/L(t)$. We find the good static and dynamic scaling in the system for disorder strengths Δ_d.

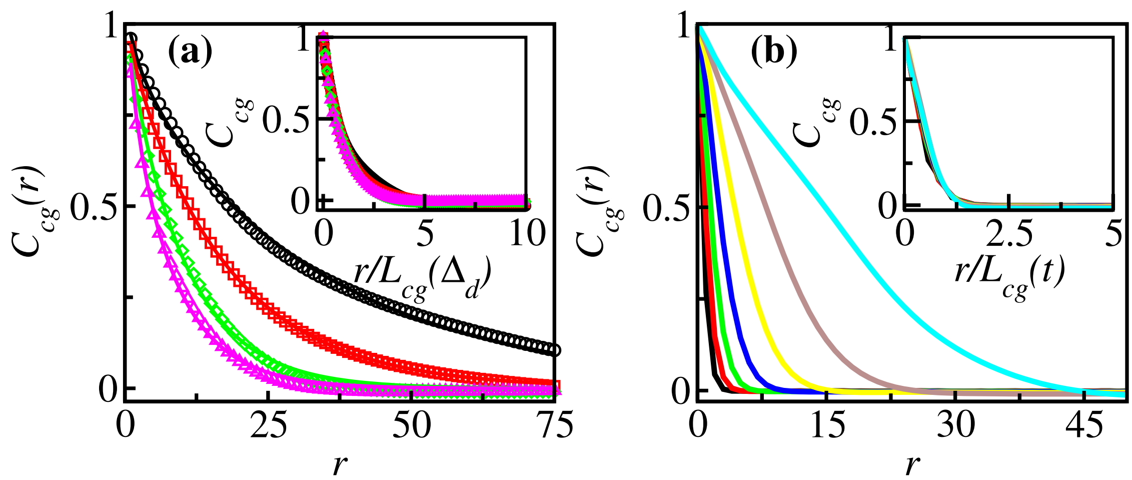

Fig. 3.7 (a) Shows the plot of two-point correlation function $C_{cg}(r)$ for various disorder strengths, Δ_d= 0.001 (black, circles), 0.002 (red, squares), 0.004 (green, diamonds), 0.007 (pink, triangles). *Inset* : The scaled $C_cg(r)$ *vs.* scaled distance $r/L(t)$. (b) shows the correlation function at different times for a particular disorder strength $\Delta_d = 0.001$. *Inset*: The scaled $C_{cg}(r)$ *vs.* scaled distance $r/L(t)$.

3.4 Conclusion

We study the effect of quenched disorder on the characteristic of self-propelled particles (SPPs) in one-dimension. The SPPs, characterized by distinct left or right orientations interact with disorder which serve as directional cues. Through extensive microscopic simulations and a numerical exploration of coarse-grained equations of motion for local density and orientation of particles, our investigation reveals how the density of the disorder influence the emergence of ordering and clustering in the collection of the SPPs. Quantifying the degree of ordering, we measure the characteristic correlation length and its corresponding exponent across varying disorder densities. The disorder affects the macroscopic ordering in the system, the size of the ordered clusters decays algebraically with disorder. Further the disorder also affects the clustering of particles, in the presence of disorder a big macroscopic cluster breaks in small clusters resulting in the increase in the number of clusters as obstacle density escalates and lead to the localisation of particles around it and ultimately resulting in high density around the disorder. Finally we can conclude that disorder splits a macroscopic globally ordered cluster to multiple localised dense clusters with different orientations. We observe identical results from the microscopic and coarse grained model.

This model can be extended to quasi one-dimension system to study the effect of disorder on the ordering of SPPs at the interface of crossover in the dimensions. Our study can help in the understanding of the confinement of mesenchymal cells to thin adhesive one-dimensional (1D) lines with a characteristic spatial force pattern Hennig et al. (2020)].